



Optimal Sizing and Energy Management of Hybrid Energy Storage System for High-Speed Railway Traction Substation

Sida Tang¹ · Xiaohong Huang¹ · Qunzhan Li¹ · Naiqi Yang¹ · Qinyu Liao¹ · Ke Sun¹

Received: 19 August 2020 / Revised: 7 December 2020 / Accepted: 22 February 2021 / Published online: 29 March 2021
© The Korean Institute of Electrical Engineers 2021

Abstract

Traction power fluctuations have economic and environmental effects on high-speed railway system (HSRS). The combination of energy storage system (ESS) and HSRS shows a promising potential for utilization of regenerative braking energy and peak shaving and valley filling. This paper studies a hybrid energy storage system (HESS) for traction substation (TS) which integrates super-capacitor (SC) and vanadium redox battery (VRB). According to the characteristics of the traction load under actual operating conditions, an energy management strategy with fixed-period control (FPC) is proposed, which fully leverages the periodicity and regularity of HSRS operation. To achieve the optimal size, economic feasibility is selected as the optimization objective, which is fully assessed in terms of Net Present Value (NPV). The optimization constraints are formulated in which the Discrete Fourier Transform (DFT) is performed for power allocation between SC and VRB. Besides, an improved mutation-based particle swarm optimization (IMBPSO) is proposed to efficiently solve the optimization and enhance convergence performance. Finally, combined with the measured traction load data, the effectiveness of the FPC energy management strategy is verified and the optimal scale of the HESS is provided.

Keywords High-speed Railway · Hybrid Energy Storage System · Fixed-period control energy management strategy · Improved particle swarm optimization

1 Introduction

China's high-speed railway construction has achieved a significant breakthrough and distinguished achievement [1]. In China, the mileage of railways in service reached 131,000 km in 2018, of which 29,000 km are high-speed lines. Meanwhile, it should be noted that the energy consumption of the railway system is high. The statistics indicated that the total energy consumption in 2018 was equivalent to 16.2 million tons of standard coal [2]. Huge energy procurement costs prompt railway system to seek a lower energy consumption. Massive actual operating data demonstrate that, for high-speed railway system (HSRS), regenerative braking energy (RBE) accounts for about 5% of total energy [3]. On the other hand, the high-speed trains (HSTs) adopt pulse width modulation (PWM)-based four-quadrant converter (four QC), thereby the regenerative braking power

(RBP) generated by the train may be up to 20 MW instantaneously [4]. Public power grid would suffer from intense impact when high-frequency power is directly fed back to the power grid. At the same time, power quality problems such as voltage imbalance, voltage reduction and frequency fluctuation are inevitably encountered [5]. Consequently, the energy storage system (ESS) has been considered as a key factor in solving these problems [6].

Energy storage utilization of regenerative braking energy in urban rail transit system has been widely applied. A case study confirms the effectiveness of reducing energy-consuming by 10% to 45% by means of regenerative braking systems [7]. Considering that the AC power supply of high-speed railway with characteristic of bi-directional energy flow, researches about energy storage and energy recycling for electrified railway have been put forward [8]9. A novel energy storage traction power supply system is examined for peak clipping and valley filling, and the validity of the control method and the excellent performance of the system are indicated by a case study in an electrified railway [10]. A co-phase traction power supply system with SC ESS was proposed in [11], and the conclusions validated that

✉ Xiaohong Huang
Huangxh_ee@swjtu.edu.cn; hxhxj924@163.com

¹ School of Electrical Engineering, SouthWest Jiaotong University, Chengdu, China

the structure effectively realized the energy management of electrified railway, including four working modes: traction, regenerative braking, peak shaving and valley filling. In [12], an ESS sizing method for peak-demand reduction of an urban railway system is proposed, and a numerical example considering data from railway systems shows the suitable performance of the ESS for railway systems. A supervision strategy based on multi-criteria approach was proposed and the results showed the good investment value of ESS in railway [13].

The energy management strategy plays an important role of reasonable configuration of ESS, and previous studies offered quite a few important insights for reference [9–13]. In [14] two different connection topologies of the ESS technologies were examined, and the system efficiency and performance were compared in an example wind farm. A knowledge-based approach was further proposed to schedule the power of a two-stage ESS, to minimize the negative impact of wind energy on the grid [15]. According to a hybrid centralized-decentralized concept, a new railway energy management system (REM-S) combining with the smart grid (SG) concept was proposed for partial energy management [16]. Based on the frame of REM-S, a prototype software suite for REM-S was developed and simulated in a suburban 3 kV DC supply railway line in Spain, where the effectiveness and reliability were validated [17]. A position-based Takagi–Sugeno fuzzy (T-S fuzzy) power management for trams equipped with ESS was proposed, and the simulation based on real traffic data indicated that the strategy allowed a 14.9% decrease in the energy consumption [18]. The management strategies proposed in above papers mostly ignored the periodicity and violent fluctuation of traction load, and simultaneously led to an excess in ESS capacity. Energy management with higher accuracy and efficiency is mandated by HSRS.

The ESS size is highly correlated with technical performance and economic investment, hence this series of problems have been attracting broad interests throughout the world. In [19] the cost–benefit analysis of ESS was formulated as a mixed linear integer problem (MLIP), in order to quantitatively determine the optimal capacity of ESS. The reliability criterion was considered further to calculate the optimal size of ESS and the problem was transformed into a mixed-integer programming (MIP) model [20]. With regard to the traction power supply system, an optimal operation model which takes the impedance of the traction network into account is brought forward, but the mixed integer non-linear programming model (MINLP) employed here involves complicated calculations. However, considering its high susceptibility to high-rate power cycling, the battery service life is also of concern [21]. For instance, a comprehensive ESS sizing model based on an MLIP of ESS was proposed, which considered the impact of depth of discharge and the

number of charging and discharging (C&D) cycles on the battery degradation [22]. The rain-flow method is generally utilized to quantitatively investigate the service life of battery [23]24. A novel bi-level of energy management system was developed based on rain-flow method, in which simulation power data of trains was employed [25]. The simulation conditions tended to be ideal, although the reduction in electricity costs demonstrated by the optimization results was satisfactory (about 30%). Likewise, the exploited algorithm has significant effects on optimization objective searching, thus an improved particle swarm optimization (PSO) is proposed in this paper.

This paper explores size optimal method and energy management strategy of hybrid energy storage system (HESS) for HSRS. An energy management strategy train-working-diagram-based is proposed by fully analyzing the daily cycle and predictability of traction load of HSRS. The HESS discharge and release energy during power peak, while charge and store energy during power valley. The HESS size problem is cast as an optimization model with the optimal objective of economic returns, where the rain-flow method is assembled for vanadium redox battery (VRB) service life evaluation. The power allocation and operation limits are formulated as optimization constraints, in which the Discrete Fourier Transform (DFT) is adopted to dispatch power between the VRB and the super-capacitor (SC). For the problems existing in the PSO solution process, an improved mutation-based particle swarm optimization (IMBPSO) incorporating the mutation-based operation is proposed to augment the global search ability and result reliability.

The rest of the paper proceeds as follows: Section II presents the energy management strategy of HESS. Section III discusses the optimal model of HESS. The results of the optimization are shown in Section IV and the related discussion is given in Section V.

2 Modeling and Scheduling of HESS

2.1 System Description

As illustrated in Fig. 1, a co-phase power supply system which mainly consists of a traction transformer system (TSS) and an active power conditioner (APC) transmits power flow from grid (i.e., P_{Grid}) to traction network (i.e., P_{Load}) [26], wherein VRB and SC are respectively connected to the APC via DC/DC converters. Generally, the length of power supply section is about 10 km, but in the HSRS equipped with co-phase power supply system the section extends to over 20 km [11]. Under the same operation condition, the TS with a longer power supply section is responsible for handling higher power flow, which shows a greater potential of HESS. When the HST is in traction mode, the HST power

Fig. 1 Traction power supply system with HESS structure

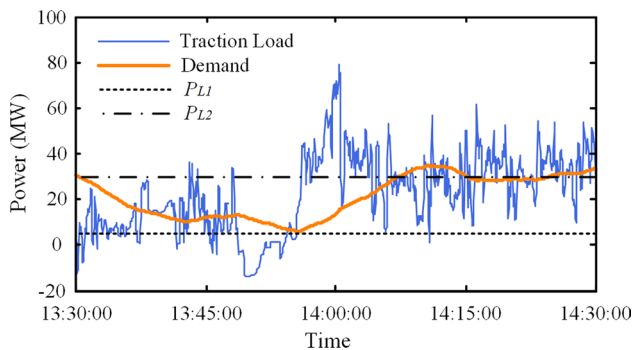
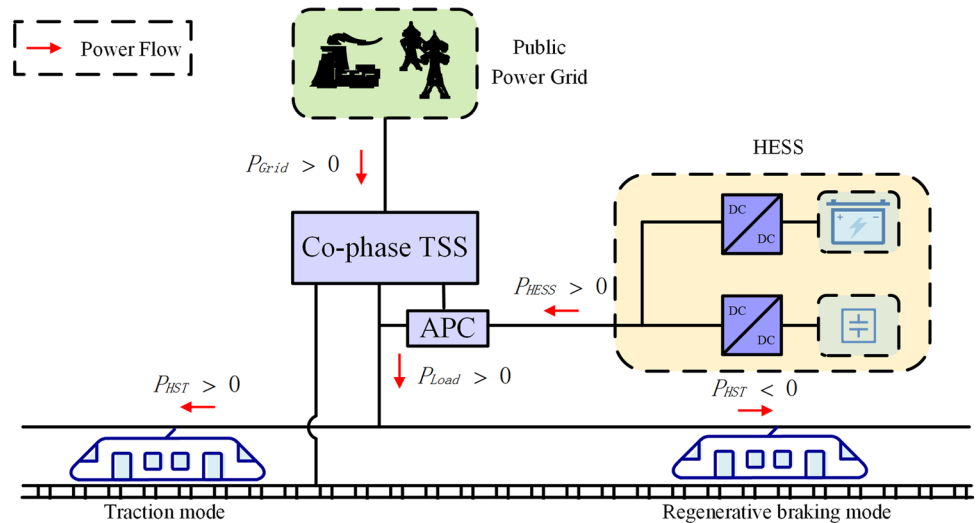


Fig. 2 Feeder traction load power curve

flow P_{HST} is greater than zero, and conversely, P_{HST} is fed back to the catenary from the HST in regenerative braking mode. As the load power exceeds the threshold region, the power flow of HESS (i.e., P_{HESS}) is responsible for peak shaving or valley filling.

The energy procurement costs of HSRs are mainly electricity bills, which consists of basic tariff and electricity tariff. It is worth noting that there are two payment modes of basic tariff, separately based on transformer capacity and maximum load demand. In realistic operating conditions, an adequate margin of transformer capacity is provided for long-term planning, therefore the mode based on maximum load demand is chosen widely. Accounting for the payment mode, HESS is exploited to reduce peak power demand and stores energy during the low load periods.

To this end, a charging threshold line P_{L1} and a discharging threshold line P_{L2} are adopted to formulate the power allocation criterion. A section of the load power and demand curve of a TS has been shown in Fig. 2. When both lines are equal to the average value of traction load, the areas of peak region and valley region are equal. It is well known

that HSTs travel according to the operation diagram which repeats every day, thereby the traction load follows the same cycle every day and is predictable in the normal condition. Based on this, an energy management strategy is proposed to realize demand reduction, and it is described in Sect. 2.2 in detail.

2.2 Energy Management Strategy

2.2.1 Fixed-Period Control Strategy

For electric utility industry, the maximum power demand tariff is deemed as an important charge pattern to maintain high efficiency of power supply equipment. Demand tariff is defined as the average power measured over a specified period (which has been appointed as 15 min by China metrological verification regulation [27]), which can be described as:

$$P_{Dem}(t) = \begin{cases} 0, & t < 0 \\ \sum_{t-\frac{900}{\Delta t}}^t P_{Load}(x), & t \geq \frac{900}{\Delta t} \end{cases} \quad (1)$$

where P_{Dem} is the demand tariff of traction load; t (s) represents the index of time.

Compared with real-time power data, power demand data filters out violent fluctuations and becomes more stable. It can be speculated that the power demand data is cyclical thanks to the daily cycle of train operation diagram. In order to verify the periodicity of the power demand, massive data of power demand are investigated, and Fig. 3 shows power demand profiles in different days.

As is illustrated in Fig. 3, the probability value of power demand is adopted as the charging threshold. And with the

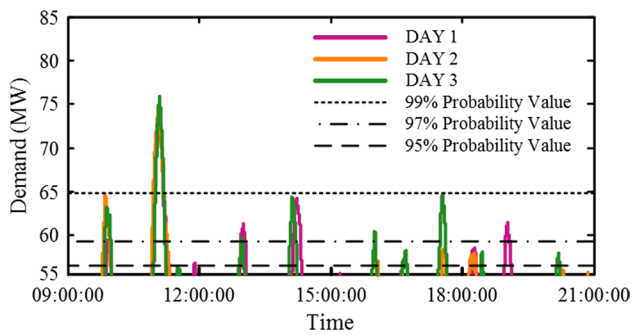


Fig. 3 Power demand curves of three days

higher threshold, the overlap degree of the curves increases. Therefore, a strategy that releases energy over a fixed time span is proposed and named fixed-period control (FPC) strategy. The historical data of power demand serving as the sample is analyzed to determine the control period. The power dispatch criterion of FPC strategy consists of 5 processes:

- i. Calculate X% probability value (typically over 80%) of sample data.
- ii. Take X% probability value of demand data as the discharging threshold P_{L2} to calculate time segment in which the power demand exceeds the discharging threshold in historical data.
- iii. Shift forward the starting point of each time horizon by 15 min as the final fixed discharge time segment.
- iv. Read the power demand data of the next day. As for time point t in the final fixed discharge time segment, if $P_{Load}(t) > MP_{L2}$, set the state of HESS as discharging. M is defined as the coefficient of peak clipping.
- v. As for time point t out of the final fixed discharge time segment, if $P_{Load}(t) < P_{L1}$, set the state of HESS as charging.

2.2.2 Real-Time Control Strategy

Another real-time control (RTC) strategy is proposed to compare the performance with the FPC strategy. As shown in Fig. 2, two threshold lines are exploited to control the load power in real-time. In comparison, the implementation of the RTC strategy is much simpler but may lead to higher capital cost.

If the traction power is greater than P_{L2} , HESS is set in discharging state. If the traction power is lower than P_{L1} , HESS is charging. In other cases, the HESS is in idle mode. It can be specifically expressed as formulas below:

$$P_{HESS}(t) = \begin{cases} P_{H,r}, P_{Load} > P_{L2} \\ 0, P_{L1} < P_{Load} \leq P_{L2} \\ P_{Load} - P_{L1}, P_{L1} - P_{H,r} < P_{Load} \leq P_{L1} \\ -P_{H,r}, P_{Load} \leq P_{L1} - P_{H,r} \end{cases} \quad (2)$$

where $P_{H,r}$ is the rated power of HESS, and $P_{HESS} > 0$ indicates HESS is discharging state.

3 Optimization of HESS Capacity

3.1 Objective Function

Onboard ESS and ESS for traction substation are two common schemes for HSRS. For onboard ESS, the effects of the vehicle operation performance are significant with the change of ESS volume and weight [28]. By contrast, traction substations are located in the suburbs with sufficient usable area, the ESS volume and weight do not constitute a major limitation [29]. Therefore, only the economic effectiveness is considered in this paper.

Cost constraints are generally used in the optimal problem of HESS capacity, where the capital cost and maintenance cost of HESS are considered. However, the HESS size also has remarkable effects on maximum demand and RBE utilization, which indicates that the economic effectiveness of the case is insufficiently analyzed by means of cost constraint. The Net Present Value (NPV) is incorporated for economic effectiveness evaluation of HESS. The objective function (i.e., NPV) of HESS sizing problem can be described as Eq. (3).

$$\begin{aligned} \min f = -NPV = & - \sum_{i=1}^{N_p} (-C_{CC}[i] - C_{MC}[i] - C_{RC}[i] \\ & + \Delta C_{EC}[i] + S_V[i]) \times (1 + F)^{-i} \end{aligned} \quad (3)$$

where N_p represents the project service period in years; $C_{CC}[i]$ refers to the cash flow of ESS capital cost; $C_{MC}[i]$ is the cash flow of operation and maintenance cost; $C_{RC}[i]$ represents the cash flow of replacement cost; $\Delta C_{EC}[i]$ is the curtailment of electricity cost; $S_V[i]$ represents the salvage value of the VRB; F refers to the annualized discount rate.

The HESS is mainly composed of VRB device, SC device and power conversion systems (PCSs), which are recognized as the central components of HESS capital cost. The capital cost of power conversion systems is related to the power level of the two energy storage devices. The cash flow of ESS capital cost can be formulated as:

$$C_{CC,ESS}[i] = \begin{cases} C_{ESS} \times E_{ESS,R} + C_{PCS} \times P_{ESS,R}, & i = 1 \\ 0, & i = 2, \dots, N_p \end{cases} \quad (4)$$

where C_{ESS} is the capital cost per unit of capacity associated with VRB and SC; C_{PCS} represents the capital cost per unit of power rating related to VRB and SC.

All through the project service period, the appropriate maintenance of energy storage devices is essential for prolonging their lifetime. The operation and maintenance cost is given as:

$$C_{MC,ESS}[i] = \begin{cases} 0, & i = 1 \\ C_{MC} \times E_{ESS,R}, & i = 2, \dots, N_p \end{cases} \quad (5)$$

where C_{MC} represents the maintenance cost per unit of capacity related to VRB and SC.

The project service period can hardly be satisfied by VRB ESS because of the limitation of number of the C&D cycles, hence the VRB ESS necessitates replacement of sulfuric acid electrolyte to keep its operational performance. And it is assumed that the operation demand can be met with the SC technology thanks to its large allowable number of C&D cycles (over 50 M). The replacement cost can be expressed as:

$$C_{RC,ESS}[i] = \begin{cases} C_{RC} \times E_{ESS,R}, & i = (1, 2, 3, \dots, k)Y_{SL} \\ 0, & i \neq (1, 2, 3, \dots, k)Y_{SL} \end{cases} \quad (6)$$

where k denotes the number of replacement times of ESS; Y_{SL} is the service lifetime of ESS in years; C_{RC} is the replacement cost per unit of capacity related to ESS.

The economic benefits generated by HESS incorporate curtailment of electricity cost. The curtailment of electricity cost is described as:

$$\Delta C_{EC}[i] = C_{EP} \times \Delta E_{EC} + C_{DCP} \times \Delta P_{Dem}, i = 1, \dots, N_p \quad (7)$$

where C_{EP} represents the electricity price of power; C_{DCP} refers to the demand charge price decided by maximum demand during a month; ΔE_{EC} and ΔP_{Dem} are the electricity consumption reduction and peak demand reduction respectively.

Considering the expected recovery value of VRB in the final year of the project service period, the salvage value S_V of the VRB can be expressed as follows.

$$S_V[i] = \begin{cases} 0, & i = 1, 2, \dots, N_p - 1 \\ C_{RC} E_{ESS,R} \frac{(k+1)Y_{SL} - N_p}{Y_{SL}}, & i = N_p \end{cases} \quad (8)$$

In order to measure the operating efficiency of the project, the return on investment (i.e. ROI) was introduced as a comprehensive indicator, which can be expressed as:

$$ROI = \frac{NPV}{\sum_{i=1}^{N_p} (C_{CC}[i] + C_{MC}[i] + C_{RC}[i])} \quad (9)$$

3.2 Problem Constraints

The optimization problem is primarily subject to the power balance, state of charge (SOC) limits and power allocation limits. The traction load, P_{Load} , should be met with the power supplied from the grid (i.e., P_{Grid}) and the power delivered by HESS (i.e., P_{HESS}) at time interval t , which can be depicted as:

$$P_{Load}(t) = P_{Grid}(t) + P_{HESS}(t) \quad (10)$$

$$P_{HESS}(t) = P_{SC}(t) + P_{VRB}(t) \quad (11)$$

where $P_{SC}(t)$ and $P_{VRB}(t)$ are the C&D power of SC and VRB respectively.

SOC limits of ESS desire consideration because of the negative effects induced by excessive C&D operations [30], which is described as Eq. (12).

$$SOC_{ESS_min} \leq SOC_{ESS}(t) \leq SOC_{ESS_max} \quad (12)$$

where $SOC_{ESS}(t)$ refer to the SOC of ESS at time interval t , respectively; SOC_{ESS_min} and SOC_{ESS_max} represent the minimum and maximum SOC of ESS.

With the advantages in power density and energy storage capacity, VRB technology becomes justifiable employment as large-capacity energy storage [31, 32], whereas its sensitivity to high-rate power cycling would negatively affect its service lifetime. To this end, SC technology is incorporated as a good complement to VRB technology due to its high power density and fast charging, thus the power coordination becomes a concomitant issue to the HESS sizing. For this problem, the DFT technology is equipped to fulfill the power allocation demand, where the goal is to dispatch low-frequency power components to VRB and deliver high-frequency power components to SC. Equation (13) and Eq. (14) indicate the mathematical formulation of DFT technology, and the HESS power sequence in the frequency domain $P_{HESS}^f[k]$ can be calculated by Eq. (13).

$$X^f[k] = \sum_{t=0}^{N-1} X^t[t] e^{-\frac{i2\pi kt}{N}}, k = 0, 1, \dots, N - 1 \tag{13}$$

$$X^t[t] = \frac{1}{N} \sum_{k=0}^{N-1} X^f[k] e^{\frac{i2\pi kt}{N}}, t = 0, 1, \dots, N - 1 \tag{14}$$

When f_p is set as the index of the cutoff frequency the power of VRB and SC, $P_{VRB}^f[k]$ and $P_{SC}^f[k]$ can be expressed as Eq. (15) and Eq. (16), in which the demarcation point (i.e., N_D) corresponds to the cutoff frequency.

$$P_{VRB}^f[k] = \left\{ \frac{1}{2} P_H^f[0], \dots, P_H^f[N_D], 0, \dots, 0, P_H^f[N - N_D], \dots, \frac{1}{2} P_H^f[0] \right\} \tag{15}$$

$$P_{SC}^f[k] = \left\{ 0, \dots, 0, P_H^f[N_D + 1], \dots, P_H^f[N - N_D - 1], 0, \dots, 0 \right\} \tag{16}$$

The ESS power sequence in time-domain (i.e. $P_{ESS}(t)$) can be calculated by Eq. (14).

3.3 Cycle Lifetime Model of VRB

It is generally believed that the number of cycle lifetime of SC can reach 500,000 – 1,000,000 times [33], which is sufficient to meet the C&D demand during the project service period. Therefore, only the service lifetime of VRB is calculated in this study. Paper [34] points out that the service lifetime of VRB is around 10 years, but it is related to many factors such as temperature, the peak C&D current and C&D times. Hence, the rain-flow method serves as an accurate calculation basis for VRB service lifetime estimation in terms of the SOC-Time curve.

With the depth of discharge (DOD) increasing, the cycle lifetime of VRB is decreased nonlinearly, thus the sum of sine method is selected as an available application for curve-fitting analysis in this study. Equation (17)

describes the VRB cycle lifetime as a function of DOD. The corresponding fitting curve is shown in Fig. 4.

$$L_C = 53130 \sin(2.21DOD + 1.32) + 49650 \sin(2.35DOD + 4.36) + 77.62 \sin(15.53DOD - 1.67) \tag{17}$$

As DOD_{base} is taken as a reference indicator, the VRB lifetime (i.e., $L_{E,i}$) consumed by a specific depth (i.e., DOD_i) can be expressed as:

$$L_{E,i} = \frac{L_{C,base}}{L_{C,i}} = \frac{L_C(DOD_{base})}{L_{C,i}(DOD_i)} \tag{18}$$

The total equivalent cycle lifetime (i.e., L) consumed during the whole operation period of VRB can be denoted as:

$$L = \sum_{i=1}^N \frac{L_C(DOD_{base})}{L_{C,i}(DOD_i)} \tag{19}$$

where N represents the number of cycles during the operation period.

3.4 Improved PSO Algorithm and Solution

For HESS sizing optimization, economic effectiveness is selected as the optimization objective and is depicted as a function of HESS rated power and capacity. Generally, optimization algorithms such as genetic algorithm (GA) and PSO are employed for the complicated optimization problem solution [35][36]. The GA for optimal solution search is available in the entire solution-space but possesses relatively low convergence speed due to the considerable calculation burden of the optimization problem. The PSO algorithm obtains improved convergence speed but can hardly avoid a local optimal solution. An IMBPSO with incorporation of crossover mutation is proposed to enhance computational efficiency and global optimization ability.

The IMBPSO algorithm starts with a group of random particles which are formulated by two decision variables, i.e., velocity V_1 and position X_1 . For each iteration, particles keep following the leading particle. The process can be expressed as:

$$V_1 = V_{min} + (V_{max} - V_{min}) \times rand \tag{20}$$

$$X_1 = X_{min} + (X_{max} - X_{min}) \times rand \tag{21}$$

$$V_{k+1} = V_k + c_1 \times rand \times (gbest - X_k) + c_2 \times rand \times (zbest - X_k) \tag{22}$$

$$X_{k+1} = X_k + V_{k+1} \tag{23}$$

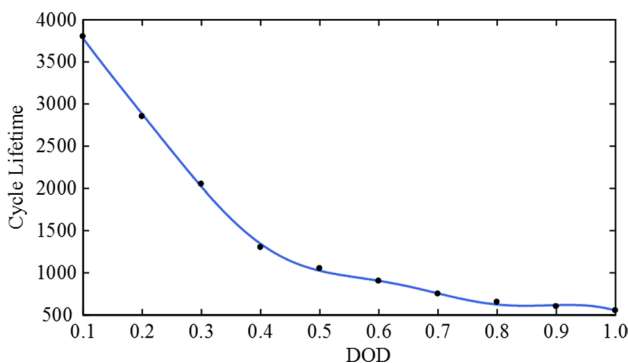


Fig. 4 Fitting curve of cycle lifetime and DOD

where V_{min} and V_{max} are the constraints of velocity; X_{min} and X_{max} are the constraints of position; $rand$ is a random vector between 0 and 1; c_1 and c_2 are learning factors; $gbest$ and $zbest$ are individual optimal value and global optimal value respectively; k refers to the index of iteration.

For promoting diversity of particle swarm and avoiding premature convergence, each particle is converted as a chromosome by binary coding under encoding constraints, the new mixed particle swarm is obtained through selection operation, crossover operation and mutation operation. The crossover mutation process is proposed as follows:

- i. Convert each particle (i.e., PSO_k) as a chromosome (i.e., $GA_k = [k_0, k_1, k_2, \dots, k_{i-1}]$) by binary coding;
- ii. Randomly select two genes and generate a random number (i.e., j) for gene segment selection. The crossover between two chosen genes with chosen segments is performed with crossover probability, repeating the operation until all the particles are investigated. The operation process can be indicated as:

$$GA_k = [k_0, k_1, k_2, \dots, k_{i-1}] \rightarrow GA_{kj} = [k_0, k_1, k_2, \dots, g_j, \dots, g_{i-1}]$$

$$GA_g = [g_0, g_1, g_2, \dots, g_{i-1}] \rightarrow GA_{gj} = [g_0, g_1, g_2, \dots, k_j, \dots, k_{i-1}]$$

- iii. A random position of chromosome is operated for mutation with mutation probability, the operation process can be expressed as:

$$GA_k = [k_0, k_1, k_2, \dots, k_{i-1}] \rightarrow GA_k^m = [k_0, k_1, k_2, \dots, k_j^m, \dots, k_{i-1}]$$

- iv. Convert each chromosome as a mutation particle (PSO_k^m);
- v. Compare the fitnesses of PSO_k and PSO_k^m (i.e. f_i and f_{mut}) calculated by Eq. (3), and preserve the particle with optimal fitness.

The dynamic procedure for the HESS sizing optimization by means of IMBPSO is illustrated in detail in Fig. 5.

4 Case Study

4.1 Case Description

To assess the performance of the proposed strategy, typical practical operation data from Danyang TS in Beijing-Shanghai HSR is analyzed, and the TS is powered by 220kV voltage with installed transformer capacity of 100 MW. The electricity price and demand charge price of the considered substation are 0.0924 USD/kWh and 6.096 USD/kWh/month respectively, also the annual discount rate is 3%. The relevant parameters of HESS are shown

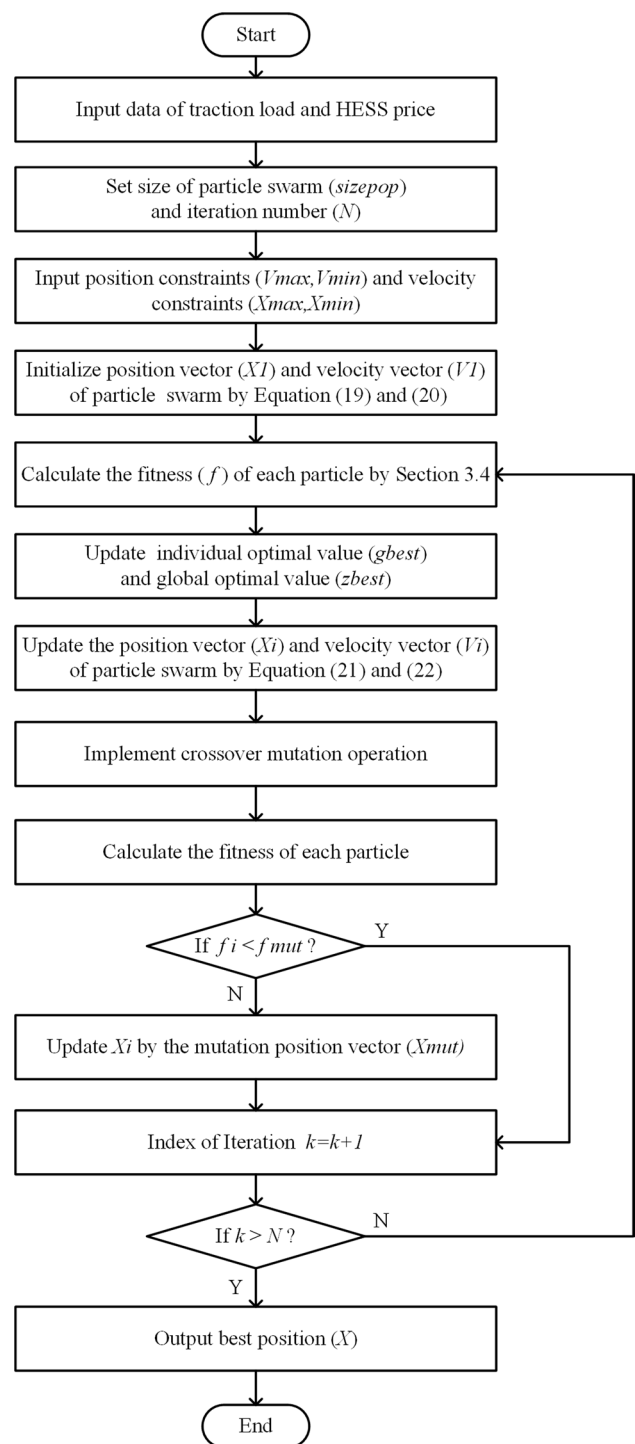


Fig. 5 Dynamic procedure for HESS sizing optimization based on IMBPSO

in Table 1 [37]. Load power and demand with sampling time interval of 1 min are illustrated in Fig. 6. The instantaneous load power fluctuated from −29MW to 94 MW with the maximum demand of 46 MVA.

The following cases are investigated:

Table 1 Parameters of HESS

Parameter	Unit	VRB	SC
Capital cost of ESS	USD/kWh	152.4	4114.8
Capital cost of PCS	USD/kW	228.6	228.6
Maintenance cost of ESS	USD/kWh	4.6	4.6
Replacement cost of ESS	USD/kWh	152.4	-
SOC range	-	10%~90%	5%~95%

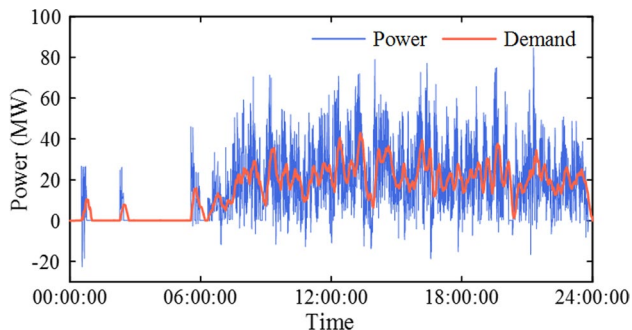


Fig. 6 Instantaneous power and demand

- Case 1: Base case.
- Case 2: Adding VRB installed RTC strategy to Case 1.
- Case 3: Adding VRB installed FPC strategy to Case 1.
- Case 4: Adding SC installed RTC strategy to Case 1.
- Case 5: Adding SC installed FPC strategy to Case 1.
- Case 6: Adding HESS installed RTC strategy to Case 1.
- Case 7: Adding HESS installed FPC strategy to Case 1.

4.2 Economic Analysis of Cases

The optimization results obtained by IMBPSO are provided in Table 2.

Case 1: as the base case, the total annualized electricity charge is 16.36 M USD without HESS, which includes demand charge of 3.36 M USD and energy consumption charge of 13 M USD.

Case 2: in this case, VRB ESS is added to the base case, and the optimal size of 13.9 MWh at 11.36 MW is found for VRB ESS by means of the proposed approach. By adding the VRB ESS, the total annualized electricity charge is 15.38 M USD, which includes 2.87 M USD demand charge and 12.52 M USD energy consumption charge. Furthermore, the VRB lead to 36.39% return on investment (ROI) during the whole project service period.

Case 3: in this case, the FPC strategy is added to case 2 for energy management. A 19.28 MWh VRB with rated power of 14.46 MW is installed with the substation. As the employment of VRB, the curtailment of the total annualized electricity charge is 1.49 M USD (i.e., 9.12% compared to the base case). Also, the VRB imposes 16.73 M USD total capital cost to the HSRS during the whole project service period and 50.81% ROI. Compared with the RTC strategy, a delightful profit is guaranteed by the FPC strategy.

Case 4: in this case, only SC ESS is added to Case1, with the optimal size of 0.4 MWh and 1.03 MW. The effects of ESS total cost reducing is significant with the application of SC ESS compared to Case 2, but it is also closely coupled with the increase in electricity charge (i.e. C_{EC}). In short, the benefit of electricity charge can hardly make up for the total cost of SC ESS.

Table 2 Optimization results of ESS sizing problem

Case No	$P_{VRB,R}$ (MW)	$E_{VRB,R}$ (MWh)	$P_{SC,R}$ (MW)	$E_{SC,R}$ (MWh)
1	-	-	-	-
2	11.36	13.9	0	0
3	14.46	19.28	0	0
4	0	0	1.03	0.4
5	0	0	3.03	0.97
6	17.01	19.44	5.8	0.11
7	18.43	19.58	6.39	0.12
Case No	HESS total cost (M USD)	C_{EC} (M USD/year)	NPV (M USD)	ROI
1	-	16.36	-	-
2	12.28	15.38	4.47	36.39%
3	16.73	14.87	8.5	50.81%
4	1.92	16.3	-0.99	-51.87%
5	4.76	16.15	-1.48	-31.8%
6	10.32	15.11	8.92	86.4%
7	10.88	14.85	12.33	113.35%

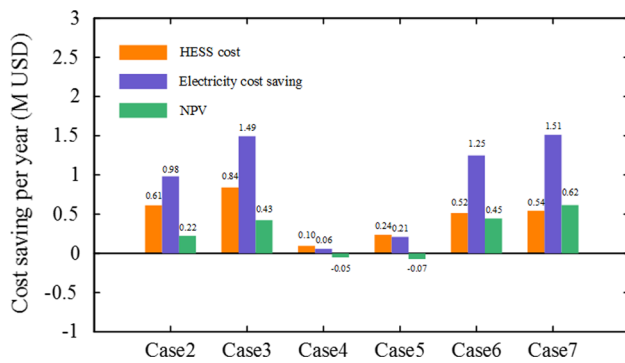


Fig. 7 Economic comparison of different cases

Case 5: A 0.97 MWh SC ESS with rated power of 3.03 MW is installed with the substation, which incurs a 1.48 M USD loss and -31.8% ROI similar to Case 4.

Case 6: SC ESS is added to Case 2, with the optimal size of 0.11 MWh and 5.8 MW. The optimal size of VRB ESS searched by IMBPSO is 19.44 MWh and 17.01 MW. The total electricity charge is reduced by 7.62% compared to that in Case 1, and the economic returns provided by HESS are 8.92 M USD during all the project service period.

Case 7: in this scenario, the FPC strategy substitutes the RTC strategy in Case 6. The optimal sizes of 19.58 MWh at 18.43 MW and 0.12 MWh at 6.39 MW are found for VRB and SC, respectively. By adding the HESS, the total annualized electricity charge is 14.85 M USD, which is reduced by 9.24% compared to that in the base case. The economic benefits provided by HESS are 12.32 M USD through all the project service period, increased by 38.28% compared to that in Case 6.

The economical comparison of different cases is intuitively demonstrated in Fig. 7. It can be seen that the FPC strategy is conducive to decreasing the electricity cost and increasing project NPV. By contrast, whatever strategy is adopted, the VRB ESS without SC ESS has a higher replacement cost and provides less economic benefits for the HSRS considering Case 2 and Case 3. Due to the high cost of SC, the cases (i.e. Case 4 and Case 5) with only SC ESS tend to choose smaller capacity, which can hardly achieve effective maximum demand reduction and further has adverse effects on economic benefits. The economic benefits augmentation of Case 6 and Case 7 reveal that the SC ESS which handles high-frequency power transients plays a vital role in system efficiency enhancement and total cost reduction. Accordingly, the maximum economic effectiveness and ROI of HESS are provided by Case 7, with an annualized benefit of 0.62 M USD and an ROI of 113.35%.

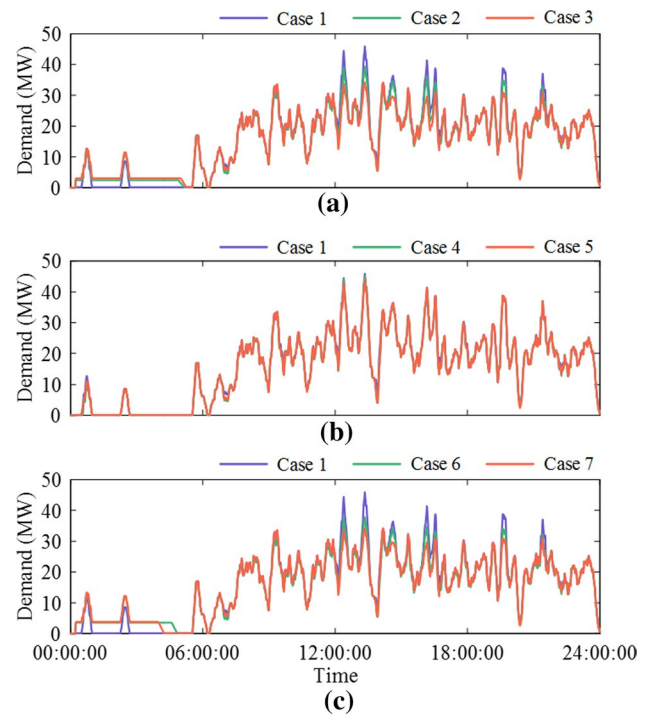


Fig. 8 Demand of substation in different cases

4.3 Performance Analysis of HESS

The HESS performance in Case 7 is in detail investigated as a typical example in this section due to the advantage of Case 7 in economic effectiveness.

Figure 8 further demonstrates the curtailment of system power demand in different ESS cases. The large-capacity VRB exhibits good capabilities of peak shaving as shown in Fig. 8a. However, In Fig. 8b, only little power demand of 1 MW is reduced due to the small capacity of the SC. In Fig. 8c, the HESS absorbs electric energy from the power grid in the period from 00:00 to 06:00, and releases electric energy during the peak period of the traction load, thus realizing the transfer of electric energy in time horizon and reducing the maximum demand.

A 17.71% reduction of maximum demand is allowed by approach obtained in Case 6, likewise, the maximum demand in Case 7 is decreased by 25.53% compared to the base case, resulting in a remarkable decrease in electricity cost. Compared to Case 6, a larger reduction of maximum demand and a higher economic benefit is obtained in Case 7. Accordingly, it can be inferred that the FPC strategy possesses higher economic viability and a more suitable operation criterion compared to the RTC strategy. It is also worth noting that although the results of system power demand reduction in Case 3 and Case 7 are similar, which is also reflected in the annualized electricity charge, but the

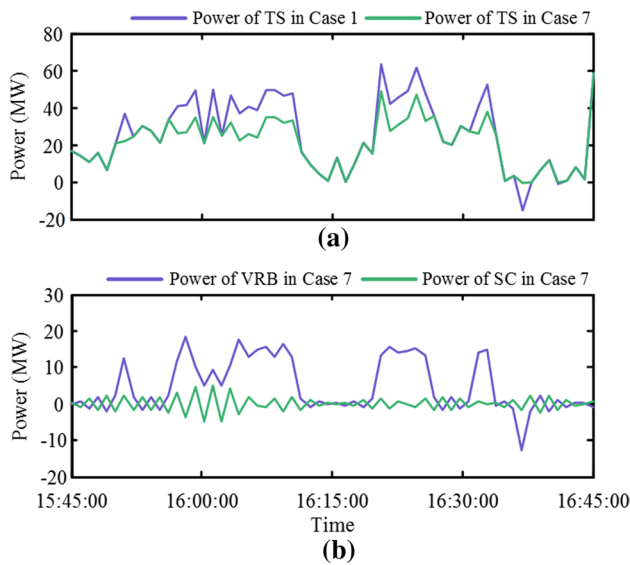


Fig. 9 (a) power of TS; (b) C&D power of VRB and SC

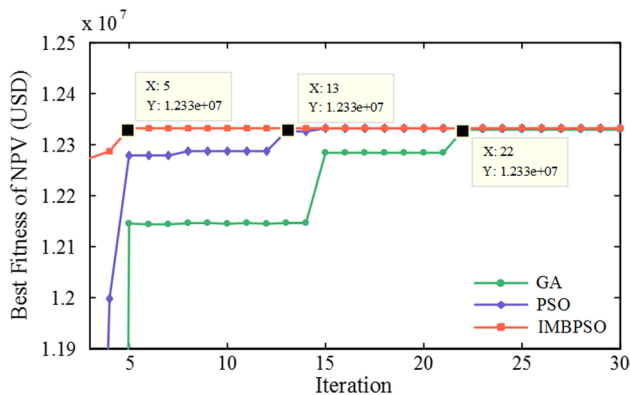


Fig. 10 Comparison of computational performance of IMBPSO, PSO and GA for Case 7

adoption of SC ESS have affects on the ESS working status, which lead to different investment costs and project NPV.

The power of TS in the base case and Case 7 at the time span from 12:30 to 15:30 are demonstrated in Fig. 9, which also depicts the C&D power of VRB and SC in Case 7 in the same period. As shown in Fig. 9a, the HESS power is negative when the TS power is lower than the charging threshold, whereas the HESS power is positive when the TS power and demand satisfied the peak shaving criterion. It can be seen that the VRB C&D process outlined in Fig. 9b possesses a smooth C&D operation and ensures the power shaving demand, meanwhile, the installed SC is conducive to alleviating the aggressive stress on VRB.

4.4 Convergence Performance of IMBPSO

In this section, both GA and PSO are exploited for solving the proposed optimization problem to compare their convergence velocity to that in IMBPSO, and Case 7 serves as an example here. Regarding the GA, the chromosome length is set as 20 with a population size of 40. As for PSO and IMBPSO, the size of particle swarm is selected as 40. For a clear demonstration of the iteration processes, only a part of them is illustrated in Fig. 10.

As is observed in Fig. 10, the optimization result of IMBPSO is achieved at the 5th iterations with best fitness of 12.33 M USD, and the PSO and GA attain the optimization solution at the 13th and 22nd iterations respectively. The best fitness obtained by PSO and GA are both 12.33 M USD. Consequently, the IMBPSO reveals a higher accuracy level and a faster convergence compared to the GA and PSO. In addition, it has shown that the proposed optimization problem is met with the PSO combined with the mutation-based method.

5 Conclusion

In this paper, an accurate optimal HESS sizing model is proposed, in which the economic viability serves as the optimization objective. For system efficiency improving, a practical energy management strategy is formulated with historical data analysis, suitable for HRSR. According to the characteristics of the proposed optimization problem, a mutation-based operation is incorporated for the PSO improvement. The feasibility of the proposed optimization model is justified through a realistic case study. The obtained conclusion can be outlined as follows:

- The efficiency of system demand curtailment and RBE recovery is enhanced with the proposed FPC energy management strategy, which allows a 31.18% ROI increase compared to RTC strategy.
- The VRB degradation is effectively subdued due to the SC application, resulting in VRB lifetime promoting and a 34.98% HESS total cost dropping.
- The proposed IMBPSO can satisfy the computational requirements of the proposed optimization problem, which also enhances the convergence performance and accuracy level due to the incorporation of the mutation-based operation.

Acknowledgements This study was supported by the research fund JHR-2019-10 from Beijing-Shanghai High Speed Railway Co., Ltd..

Funding Not applicable.

Declarations

Conflicts of interest Not applicable.

References

- Li Q. (2016). Industrial frequency single-phase AC traction power supply system for urban rail transit and its key technologies. *J Mod Transport*.
- Ministry of Transport of the People's Republic of China. (2019). Bulletin of Statistics for the Chinese Railways in 2019. Mot Gov Web. <http://www.mot.gov.cn/tongjishuju/tielu/202005/P020200511352537906795.pdf>
- Ratniyomchai T, Tricoli P, Hillmansen S (2014) Recent developments and applications of energy storage devices in electrified railways. *IET Electrical Systems in Transportation* 4(1):9–20
- Wang K, Hu H, Zheng Z, He Z, Chen L (2018) Study on Power Factor Behavior in High-Speed Railways Considering Train Timetable. *IEEE Transactions on Transportation Electrification* 4(1):220–231
- Paatero JV, Lund PD (2007) Effects of large-scale photovoltaic power integration on electricity distribution networks. *Renewable Energy* 32(2):216–234
- Jaafar A, Akli CR, Sareni B, Roboam X, Jeunesse A (2009) Sizing and Energy Management of a Hybrid Locomotive Based on Flywheel and Accumulators. *IEEE Trans Veh Technol* 58(8):3947–3958
- Gonzalez-Gil A, Palacin R, Batty P (2013) Sustainable urban rail systems: strategies and technologies for optimal management of regenerative braking energy. *Energy Convers Manage* 75:374–388
- Hernandez JC, Sutil FS (2016) Electric vehicle charging stations fed by renewable: PV and train regenerative braking. *IEEE Lat Am Trans* 14(7):3262–3269
- Chen M, Li Q, Hillmansen S et al (2016) Modelling and performance analysis of advanced combined co-phase traction power supply system in electrified railway. *IET Gener Transm Distrib* 10(4):906–916
- Chen M, Cheng Y, Cheng Z, Zhang D, Lv Y, Liu R (2020) Energy Storage traction power supply system and control strategy for an electrified railway. *IET Gener Transm Distrib* 14(12):2304–2314
- Huang X, Liao Q, Li Q, Tang S, Sun K (2020) Power management in co-phase traction power supply system with super capacitor energy storage for electrified railways. *Railway Eng Sci* 28(1):85–96
- Rakkyung K, Hyung-Chul J, Sung-Kwan J (2019) Energy storage system capacity sizing method for peak-demand reduction in urban railway system with photovoltaic generation. *J Electr Eng Technol* 14:1771–1775
- Pankovits P, Abbas D, Saudemont C et al (2016) Multi-Criteria fuzzy-logic optimized supervision for hybrid railway power substations. *Math Comput Simulat* 130:236–250
- Li W, Joos G (2007) Comparison of Energy Storage System Technologies and Configurations in a Wind Farm. In: 2007 *IEEE Power Electronics Specialists Conference*, 17–21 June 2007. pp 1280–1285.
- Abbey C, Strunz K, Joos G (2009) A knowledge-based approach for control of two-level energy storage for wind energy systems. *IEEE Trans Energy Convers* 24(2):539–547
- Khayyam S et al (2016) Railway energy management system: centralized–decentralized automation architecture. *IEEE Trans Smart Grid* 7(2):1164–1175
- Razik L, Berr N, Khayyam S, Ponci F, Monti A (2019) REM-S–railway energy management in real rail operation. *IEEE Trans Veh Technol* 68(2):1266–1277
- Talla J, Streit L, Peroutka Z, Drabek P (2015) Position-based T-S fuzzy power management for tram with energy storage system. *IEEE Trans Industr Electron* 62(5):3061–3071
- Chen S., Gooi HB., Wang M. Sizing of energy storage for microgrids. In: 2012 IEEE Power and Energy Society General Meeting, 22–26 July 2012 2012. pp 1–1.
- Bahramirad S, Reder W, Khodaei A (2012) Reliability-constrained optimal sizing of energy storage system in a microgrid. *IEEE Transactions on Smart Grid* 3(4):2056–2062
- Zhang L, Hu X, Wang Z, Sun F, Deng J, Dorrell DG (2018) Multi-objective optimal sizing of hybrid energy storage system for electric vehicles. *IEEE Trans Veh Technol* 67(2):1027–1035
- Alsaidan I, Khodaei A, Gao W (2018) A comprehensive battery energy storage optimal sizing model for microgrid applications. *IEEE Trans Power Syst* 33(4):3968–3980
- Amzallag C, Gery J, Robert J, Bahuaud J (1994) Standardization of the rainflow counting method for fatigue analysis. *Int J Fatigue* 16(4):287–293
- Bordin C, Anuta HO, Crossland A, Gutierrez IL, Dent CJ, Vigo D (2017) A linear programming approach for battery degradation analysis and optimization in offgrid power systems with solar energy integration. *Renew Energy* 101:417–430
- Liu Y, Chen M, Lu S et al (2018) Optimized sizing and scheduling of hybrid energy storage systems for high-speed railway traction substations. *Energies* 11:2199
- Qunzhan L., Wei L., Zeliang S., Shaofeng X., Fulin Z. (2014) Co-phase power supply system for HSR. In: 2014 International Power Electronics Conference (IPEC-Hiroshima 2014—ECCE ASIA), 18–21 May 2014. pp 1050–1053.
- National Electromagnetic Metrology Technical Committee (2010) Electricity meters with maximum demand measurement functions JIG 569–2014. China Quality and Standards Publishing & Media Co., Ltd, Beijing
- Chaoxian W, Shaofeng L, Fei X, Lin J, Minwu C (2020) Optimal sizing of onboard energy storage devices for electrified railway system. *IEEE Trans Transport Electrification* 6(3):1301–1311
- Sengor I, Kilickiran HC, Akdemir H et al (2018) Energy management of a smart railway station considering regenerative braking and stochastic behaviour of ESS and PV generation. *IEEE Trans Sustain Energy* 9(3):1041–1050
- Jafari M, Gauchia A, Zhang K, Gauchia L (2015) Simulation and Analysis of the effect of real-world driving styles in an ev battery performance and aging. *IEEE Trans Transport Electrification* 1(4):391–401
- Khaligh A, Li Z (2010) Battery, ultracapacitor, fuel cell, and hybrid energy storage systems for electric, hybrid electric, fuel cell, and plug-in hybrid electric vehicles: state of the art. *IEEE Trans Veh Technol* 59(6):2806–2814
- Zou Y, Li SE, Shao B, Wang B (2016) State-space model with non-integer order derivatives for lithium-ion battery. *Appl Energy* 161:330–336
- Hameer S, van Niekerk JL (2015) A review of large-scale electrical energy storage. *Int J Energy Res* 39(9):1179–1195
- Poullikkas A (2013) A comparative overview of large-scale battery systems for electricity storage. *Renew Sustain Energy Rev* 27:778–788
- Yang Z, Yang Z, Xia H, Lin F, Zhu F (2017) Supercapacitor State based control and optimization for multiple energy storage devices considering current balance in urban rail transit. *Energies* 10(4):520

36. Pankovits P., Pouget J., Robyns B., Delhaye F., Brisset S. (2014). Towards railway-smartgrid: Energy management optimization for hybrid railway power substations. In: IEEE PES Innovative Smart Grid Technologies, Europe, 12–15 Oct. 2014. pp 1–6.
37. Jiazhi L, Qingwu G, Jinhong L et al (2019) Optimal allocation of a VRB energy storage system for wind power applications

considering the dynamic efficiency and life of VRB in active distribution networks. IET Renew Power Gener 13(4):563–571

Publisher's Note Springer Nature remains neutral with regard to jurisdictional claims in published maps and institutional affiliations.